Variation from number- to chaotic-state fields: A generalized geometric state

A.-S. F. Obada
Mathematics Department, Faculty of Science, Al-Azhar University, Nasr City, Cairo, Egypt

S. S. Hassan*
Mathematics Department, Faculty of Science, Ain Shams University, Cairo, Egypt

R. R. Puri
Theoretical Reactor Physics Section, Bhabha Atomic Research Center, Bombay 400-085, India

M. Sebawe Abdalla
Mathematics Department, College of Science, King Saud University, P.O. Box 2455, Riyadh 11451, Saudi Arabia
(Received 23 November 1992)

We introduce a formal state of the radiation field which interpolates between the (pure) number (Fock) state and the (nonpure) chaotic state. The correlation functions and the squeezing properties are studied. The study of two quantum optical systems (namely, the Jaynes-Cummings model and resonance fluorescence for a single atom and many cooperative atoms) in such a state of the radiation field provides more insight into the gradual behavior as one goes from the number state to the chaotic state. A scheme for the production of such a state is sought to be realized in a model of multiphoton processes in a finite-level atomic system. The quasiprobability Wigner distribution function for such a state is also examined.

PACS number(s): 42.50.Dv, 42.50.Ar, 42.50.Md

I. INTRODUCTION

The number (Fock) state $|n\rangle$ of the radiation field is of fundamental importance to the concept of the photon in the quantum theory of radiation [1]. Any general pure photon state of the quantized radiation field is expressed as a linear combination of the basic states $|\{n\}\rangle$. For example, the single-mode coherent state $|\alpha\rangle$ is a Poisson distribution of the number states with a mean photon number $|\alpha|^2$ [2,3]. In fact, the states $|n\rangle$ and $|\alpha\rangle$ are widely used bases for representation of the radiation field.

For nonpure (mixed) states, an important example is the chaotic radiation state. For the single-mode case, the field density operator in the P representation is defined by [2,3]

$$\hat{\rho}_{\rm ch}=\int d^2\alpha\, P(\alpha)|\alpha\rangle\langle\alpha| \ , \tag{1.1}$$

where P is the Gaussian function,

$$P(\alpha)=(\pi|\alpha|^2_{\rm av})^{-1}\exp(-|\alpha|^2/|\alpha|^2_{\rm av}) \ , \tag{1.1'}$$

where $|\alpha|^2_{\rm av}=\bar{n}$ is the mean photon number in the relevant mode. For the special case of thermal (blackbody) field of frequency ω

$$|\alpha|^2_{\rm av}=(e^{\hbar\omega/\kappa_B T}-1)^{-1} \ , \tag{1.2}$$

with $K_B T$ its thermal energy.

In terms of the number states, $\hat{\rho}_{\rm ch}$ is given by [2,3]

$$\hat{\rho}_{\rm ch}=\frac{1}{1+\bar{n}}\sum_{n=0}^{\infty}\left[\frac{\bar{n}}{1+\bar{n}}\right]^n|n\rangle\langle n|=\sum_{n=0}^{\infty}p_n|n\rangle\langle n| \ , \tag{1.3}$$

where $p_n=(\bar{n})^n/(1+\bar{n})^{1+n}$ is the Bose-Einstein *(geometric)* distribution function.

Recently, Stoler, Saleh, and Teich [4] have introduced the (pure) binomial state of the radiation field which interpolates between the number state $|n\rangle$ and the coherent state $|\alpha\rangle$. For a certain range of parameters antibunching and squeezing properties of the binomial states are exhibited. The possibility for physical realization for this state was discussed by Dattoli, Gallardo, and Torre [5]. Also, negative binomial states for the field (i.e., states with negative binomial distribution) have been studied [6].

The purpose of the present work is to study the gradual behavior of some quantum optical systems where the state of the radiation field changes from the pure number state $|n\rangle$ to the (nonpure) chaotic state. This can be done through the formal introduction of a field state that interpolates between the number and the chaotic states. We call this intermediate state a *generalized geometric state,* and it reduces to each with the proper limits.

The paper is planned as follows. In Sec. II we introduce the generalized geometric state and discuss its properties (bunching; squeezing). In Sec. III we discuss two specific examples of quantum systems, namely, the Jaynes-Cummings model and resonance fluorescence. In Sec. IV we calculate the quasiprobability functions for such states. This is followed by a scheme for producing such states in Sec. V. Some concluding remarks follow in Sec. VI.

II. GENERALIZED GEOMETRIC STATE

A. Definition

We define the normalized generalized geometric state as

$$|Y,M\rangle=\lambda_0\sum_{n=0}^{M}Y^{n/2}|n\rangle\ , \tag{2.1}$$

where Y is a complex parameter and its phase is random in general and the normalization constant is

$$|\lambda_0|^2=\frac{1-|Y|}{1-|Y|^{M+1}}\ ,\quad |Y|\neq 1\ . \tag{2.2}$$

The limiting cases of the definition in (2.1) follow.

(a) Chaotic state. For $|Y|<1$ $(=\bar{n}/(1+\bar{n})]$ and $M\rightarrow\infty$, the density operator in this case is

$$\hat{\rho}_{Y,\psi}=\lim_{M\rightarrow\infty}|Y,M\rangle\langle Y,M|$$

$$=\lim_{M\rightarrow\infty}|\lambda_0|^2\sum_{n,n'=0}^{\infty}Y^{n/2}Y^{*n'/2}|n\rangle\langle n'|\ . \tag{2.3}$$

If $Y=|Y|e^{2i\psi}$ and ψ is a random phase, then the average over ψ gives

$$(\hat{\rho}_{Y,\psi})_{\rm av}=\frac{1}{2\pi}\int_0^{2\pi}\hat{\rho}_{Y,\psi}d\psi$$

$$=\frac{1}{1+\bar{n}}\sum_{n,n'=0}^{\infty}|Y|^{(n+n')/2}\frac{1}{2\pi}\times\int_0^{2\pi}e^{i(n-n')\psi}d\psi|n\rangle\langle n'|$$

$$=\sum_{n=0}^{\infty}\frac{(\bar{n})^n}{(1+\bar{n})^{n+1}}|n\rangle\langle n|\ . \tag{2.4}$$

This is identical with $\hat{\rho}_{\rm ch}$ of (1.3) for the single-mode chaotic state with mean photon number $\bar{n}$.

(b) The number state. For $|Y|\rightarrow\infty$ and M finite, Eq. (2.1) reduces to the number state $|M\rangle$.

(c) The vacuum state $|0\rangle$. This is either obtained by taking the limit $|Y|\rightarrow 0$ or equivalently by taking $M=0$.

B. Properties

The mean value for the mth moment of the photon number operator in the generalized geometric state is given by

$$\langle\hat{n}^m\rangle=|\lambda_0|^2\sum_{n=0}^{M}n^m|Y|^n\ . \tag{2.5}$$

In particular, for $m=1,2$ we have

$$\langle\hat{n}\rangle=|\lambda_0|^2\sum_{n=0}^{M}n|Y|^n$$

$$=|Y|(1-|Y|)^{-1}(1-|Y|^{M+1})^{-1}\times[1-(M+1)|Y|^M+M|Y|^{M+1}] \tag{2.6}$$

and

$$\langle\hat{n}^2\rangle=|\lambda_0|^2\sum_{n=0}^{M}n^2|Y|^n$$

$$=(1-|Y|)^{-2}(1-|Y|^{M+1})^{-1}\times[|Y|(1+|Y|)-(M+1)^2|Y|^{M+1}+(2M^2+2M-1)|Y|^{M+2}-M^2|Y|^{M+3}]\ . \tag{2.7}$$

Note that from (2.6) and (2.7) we have in the chaotic-state limit $\langle\hat{n}\rangle\rightarrow\bar{n}$ and $\langle\hat{n}^2\rangle\rightarrow\bar{n}(2\bar{n}+1)$, and in the number-state $|M\rangle$ limit $\langle\hat{n}\rangle\rightarrow M$, and $\langle\hat{n}^2\rangle\rightarrow M^2$.

The normalized second-order correlation function is defined by

$$g^{(2)}(0)=\frac{\langle a^{\dagger 2}a^2\rangle}{\langle a^\dagger a\rangle^2}=\frac{\langle\hat{n}^2\rangle-\langle\hat{n}\rangle}{\langle\hat{n}\rangle^2}\ ,$$

where a and $a^\dagger$ are the annihilation and creation field operators with algebra $[a,a^\dagger]=1$.

Thus, the use of (2.6) and (2.7) gives

$$g^{(2)}(0)=(1-|Y|^{M+1})[1+M|Y|^{M+1}-(M+1)|Y|^M]^{-2}\times[2-M(M+1)|Y|^{M-1}+2(M^2-1)|Y|^M-M(M-1)|Y|^{M+1}]$$

$$\rightarrow\begin{cases}2 & \text{for chaotic state}\\ (1-1/M) & \text{for the number state } |M\rangle\end{cases}\ . \tag{2.8}$$

For the special case of $M=1$, $g^{(2)}(0)=0$, an expected result since the state $|Y,1\rangle$ does not contain in its expansion the photon number state $|2\rangle$. Figures 1(a) and 1(b) show the behavior of $g^{(2)}(0)$ against $|Y|<1$. For $M=2$ [Fig. 1(a)], $0.69<g^{(2)}(0)\leq 1.94$. In the range $0<|Y|<0.36$, there is a partial coherent property $[g^{(2)}(0)>1]$. For $0.36<|Y|<0.9$ the antibunching effect $[g^{(2)}(0)<1]$ is clear—but it is less compared with the photon number state $[g^{(2)}(0)=\frac{1}{2}$ for the state $|2\rangle]$. For higher values of $M=10$, the chaotic behavior is exhibited $[g^{(2)}(0)=2]$ for $|Y|<0.3$ [Fig. 1(b)]. In fact as $M\rightarrow 100$, $g^{(2)}(0)=2$ for the whole range of $0<|Y|<0.95$.

The ratio of the variance function of the photon number $(\Delta\hat{n})^2$ to the mean photon number (the Fano factor) is defined as

$$F=\frac{(\Delta\hat{n})^2}{\langle\hat{n}\rangle}=\frac{\langle\hat{n}^2\rangle-\langle\hat{n}\rangle^2}{\langle\hat{n}\rangle}\ . \tag{2.9}$$

(For a number state, $F=0$.)

In the special case of $M=1$,

$$F=1-\frac{|Y|}{1+|Y|}=\frac{1}{1+|Y|}<1\ , \tag{2.10}$$

the generalized geometric distribution shows sub-Poissonian behavior [Fig. 2(a)]. For $M=2$ [Fig. 2(b)] the sub-Poissonian behavior is shown in the range $0.37\leq|Y|<0.9$. The cases of $M=10,100$ [Figs. 2(c) and

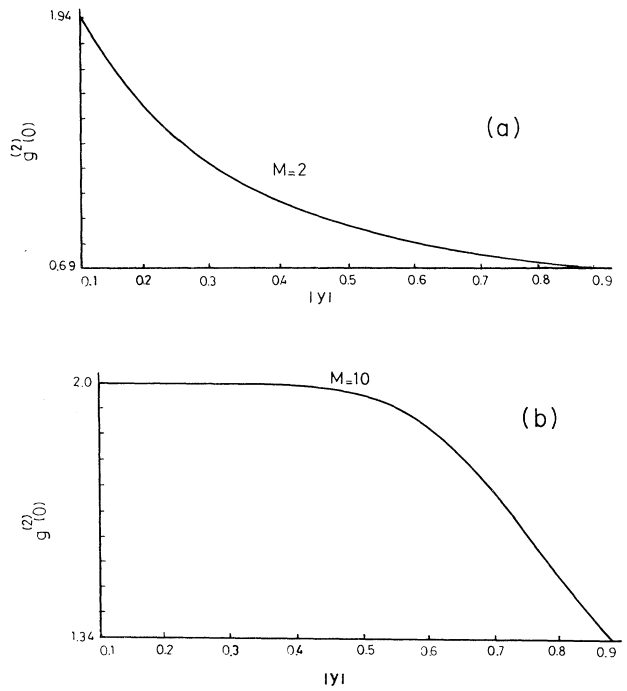

FIG. 1. The normalized second-order correlation function $g^{(2)}(0)$ against $|Y|$ (<1) (a) for $M=2$ and (b) for $M=10$.

2(d)] indicate the chaotic character of the state ($F>1$).

Now to examine the squeezing property of the generalized geometric state, we define the two quadrature components for the field (namely, the position and momentum operators)

$$\hat{X}=\frac{1}{\sqrt{2}}(a+a^{\dagger}) ,$$
$$\hat{P}=\frac{1}{\sqrt{2}i}(a-a^{\dagger}) . \tag{2.11}$$

Thus the variances $(\Delta\hat{X})^2\equiv\langle\hat{X}^2\rangle-\langle\hat{X}\rangle^2$ and $(\Delta\hat{P})^2$ are expressed as

$$(\Delta X)^2=\tfrac{1}{2}\langle a^2+a^{\dagger 2}\rangle+\langle\hat{n}\rangle+\tfrac{1}{2}-\tfrac{1}{2}\langle a+a^{\dagger}\rangle^2 ,$$
$$(\Delta\hat{P})^2=-\tfrac{1}{2}\langle a^2+a^{\dagger 2}\rangle+\langle\hat{n}\rangle+\tfrac{1}{2}+\tfrac{1}{2}\langle a-a^{\dagger}\rangle^2 . \tag{2.12}$$

From the definition (2.1), we get

$$\begin{aligned}\langle a^2\rangle&=\langle Y,M|a^2|Y,M\rangle\\&=|\lambda_0|^2\sum_{n,n'}Y^{n/2}Y^{*n'/2}\sqrt{n(n-1)}\delta_{n',n-2}\\&=|\lambda_0|^2(Y^*)^{-1}\sum_{n=2}^{M}|Y|^n\sqrt{n(n-1)}\\&=\langle a^{\dagger 2}\rangle^* .\end{aligned} \tag{2.13}$$

Hence,

$$\langle a^2+a^{\dagger 2}\rangle=2|\lambda_0|^2|Y|^{-2}\cos(\phi)\sum_{n=2}^{M}\sqrt{n(n-1)}|Y|^n , \tag{2.13'}$$

where

$$Y=|Y|e^{i\phi}\quad(\phi=2\psi) .$$

Also, we can show that

$$\langle a+a^{\dagger}\rangle=2|\lambda_0|^2|Y|^{-1/2}\cos\left[\frac{\phi}{2}\right]\sum_{n=1}^{M}\sqrt{n}\,|Y|^n , \tag{2.14}$$

$$\langle a-a^{\dagger}\rangle=2i|\lambda_0|^2|Y|^{-1/2}\sin\left[\frac{\phi}{2}\right]\sum_{n=1}^{M}\sqrt{n}\,|Y|^n .$$

The numerical results for the variance expressions,

$$S_1=2(\Delta X)^2-1 ,$$
$$S_2=2(\Delta P)^2-1 , \tag{2.15}$$

where $S_{1,2}<0$ signify squeezing, are presented in Figs. 3(a)–3(c). In the case $M=1$ [Fig. 3(a)], the component S_1 shows squeezing for $\phi=0$ up to $|Y|\simeq 0.98$, but for $\phi=\pi/4$ a lesser squeezing occurs for shorter range of $|Y|$

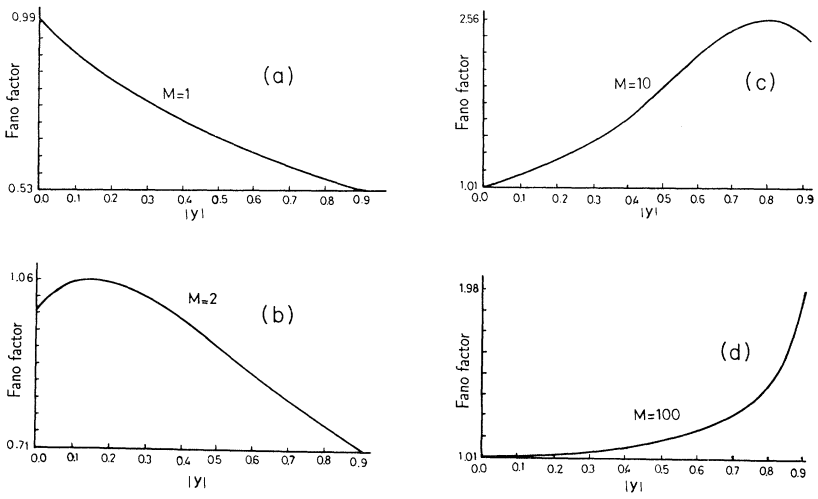

FIG. 2. The Fano factor $(\Delta\hat{n})^2/\langle\hat{n}\rangle$ against $|Y|$ (<1) (a) for $M=1$, (b) $M=2$, (c) $M=10$, and (d) $M=100$.

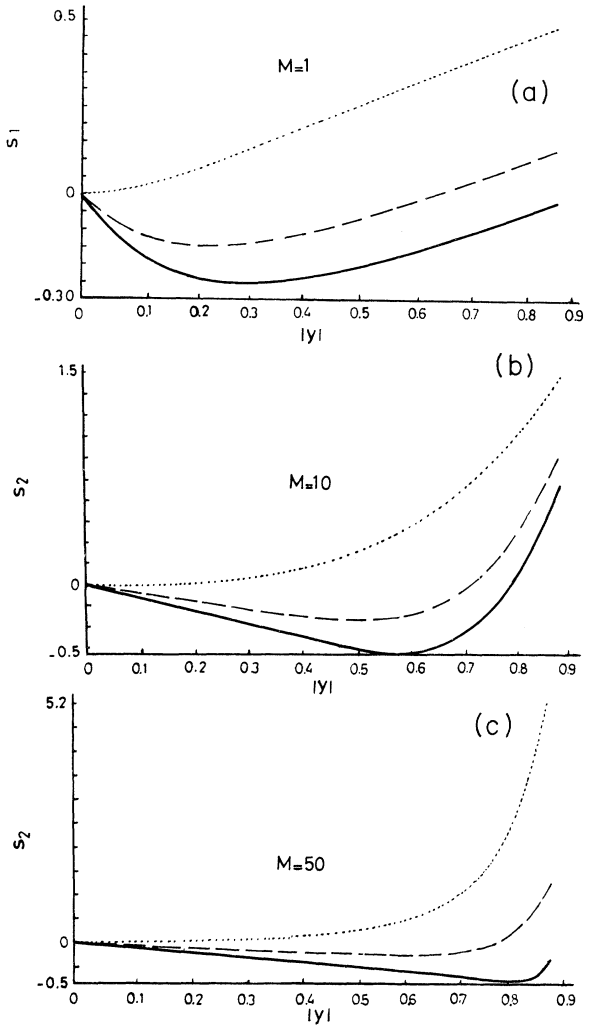

FIG. 3. (a) The variance $S_1=2(\Delta X)^2-1$ against $|Y|$ (<1) for $M=1$ and different phases $\phi=0$ (——), $\phi=\pi/4$ (– – – –) and $\phi=\pi/2$ (.....). (b) The variance $S_2=2(\Delta P)^2-1$ for $M=10$. (c) The same as (b) for $M=50$.

(namely, $0<|Y|\leq 0.7$). There is no squeezing at all for $\phi=\pi/2$. In conformity with the case $M=1$, the component S_2 does not exhibit squeezing for the same values of ϕ. For $M=10$, S_2 shows some squeezing for $\phi=0,\pi/4$ [Fig. 3(b)]. The same is true for the case $M=50$, but the magnitude of squeezing is less [Fig. 3(c)]. In both cases of $M=10$ and 50 there is no squeezing in S_1 as expected.

Note that for $|Y|\gg 1$, both $S_{1,2}$ are positive for all ϕ, hence there is no squeezing. This is consistent with the fact that as $|Y|\rightarrow\infty$ the generalized geometric state tends to a Fock (number) state which does not exhibit squeezing in $S_{1,2}$.

III. EXAMPLES OF QUANTUM OPTICAL SYSTEMS

In order to understand the behavior of some quantum systems, where the state of the radiation field changes from the number to the chaotic state, we express the density operator for the generalized geometric state either in terms of the number states $|n\rangle$ or the coherent state $|\alpha\rangle$. So,

$$\hat{\rho}_{Y,M}=|Y,M\rangle\langle Y,M| =|\lambda_0|^2\sum_{n,n'=0}^{M}Y^{n/2}Y^{*n'/2}|n\rangle\langle n'| \ . \tag{3.1a}$$

If $Y=|Y|e^{2i\psi}$ and then we average over the phase ψ, we get

$$(\hat{\rho}_{Y,M})_{\rm av}=\frac{1}{2\pi}\int_0^{2\pi}\hat{\rho}_{Y,M}d\psi =|\lambda_0|^2\sum_{n=0}^{M}|Y|^n|n\rangle\langle n| \ . \tag{3.1b}$$

Hence, for an operator $\hat{O}$, the expectation value in the $|Y,M\rangle$ state is given by

$$\langle\hat{O}\rangle_{Y,M}=\langle Y,M|\hat{O}|Y,M\rangle =|\lambda_0|^2\sum_{n=0}^{M}|Y|^n\langle n|\hat{O}|n\rangle \ . \tag{3.2}$$

Also, we may express the density operator $|n\rangle\langle n|$ for the number state in terms of that for the (single-mode) coherent state $|\alpha\rangle\langle\alpha|$ by the formula [7,8]

$$|n\rangle\langle n|=\int\frac{d^2\alpha}{\pi}\sum_{m=0}^{n}\frac{n!}{(m!)^2(n-m)!}\frac{\partial^{2m}}{\partial\alpha^m\partial\alpha^{*m}} \times\delta(\alpha)\delta(\alpha^*)|\alpha\rangle\langle\alpha| \ . \tag{3.3}$$

Hence from (3.1b) and (3.3) we get

$$\langle\hat{O}\rangle_{Y,M}=|\lambda_0|^2\sum_{n=0}^{M}|Y|^n\int\frac{d^2\alpha}{\pi}\delta(\alpha)\delta(\alpha^*) \times\sum_{m=0}^{n}\frac{n!}{(m!)^2(n-m)!} \times\frac{\partial^{2m}\langle\hat{O}\rangle_\alpha}{\partial\alpha^m\partial\alpha^{*m}} \ , \tag{3.4}$$

where $\langle\hat{O}\rangle_\alpha=\langle\alpha|\hat{O}|\alpha\rangle$ is the expectation value in the $|\alpha\rangle$ state.

Note that form (3.2) is valid for a phase-averaged form of the states $|Y,M\rangle$. It will hold as well for any phase ψ if the operator $\hat{O}$ connects only the diagonal elements. In general for a non-phase-averaged state we have

$$\langle\hat{O}\rangle_{Y,M}=|\lambda_0|^2\sum_{n,n'=0}^{M}Y^{n/2}Y^{*n'/2}\langle n'|\hat{O}|n\rangle \ . \tag{3.2'}$$

Also Eq. (3.4) is valid for phase-averaged state $|Y,M\rangle$ and it holds for any phase ψ if only $\langle\hat{O}\rangle_\alpha$ is a function of $|\alpha|^2$. Otherwise, (3.3) and (3.4) are generalized to

$$|n'\rangle\langle n|=\pi^{-1}\int d^2\alpha\,P(\alpha,\alpha^*)|\alpha\rangle\langle\alpha| \ , \tag{3.3'}$$

where

$$P(\alpha,\alpha^*)=\sum_{m=0}^{n}\frac{\sqrt{n'!n!}(-)^{n'-n}}{(n-m)!m!(n'-n+m)!} \times\frac{\partial^m}{\partial\alpha^{*m}}\frac{\partial^{n'-n+m}}{\partial\alpha^{n'-n+m}}\delta(\alpha)\delta(\alpha^*)$$

and

$$\langle \hat{O} \rangle_{Y,M} = |\lambda_0|^2 \sum_{n,n'=0}^{M} Y^{n/2} Y^{*n'/2} \int \pi^{-1} d^2\alpha \, \delta(\alpha)\delta(\alpha^*) \sum_{m=0}^{n} \frac{\sqrt{n'!n!}(-)^{n'-n}}{(n-m)!m!(n'-n+m)!} \frac{\partial^m}{\partial \alpha^{*m}} \frac{\partial^{n'-n+m}}{\partial \alpha^{n'-n+m}} \langle \hat{O} \rangle_{\alpha} . \quad (3.4')$$

We now examine the effect of the gradual change of the radiation field state from number to chaotic states in two fundamental quantum optical models.

Example 1. The Jaynes-Cummings model. The Jaynes-Cummings (JC) model [9] describes the interaction of a single two-level atom with a single mode of the radiation field inside a lossless cavity (idealized high-Q cavity). The JC Hamiltonian in the rotating wave approximation and at exact resonance is given by (units of $\hbar = 1$)

$$H = \omega a^{\dagger} a + \omega S_z + g(a^{\dagger} S_- + S_+ a) , \quad (3.5)$$

where $a, a^{\dagger}$ are the field annihilation and creation operators, the atom is described by the spin-$\frac{1}{2}$ Pauli operators $S_{\pm,z}$, and g is the coupling constant.

For the radiation field initially in number state $|n\rangle$ and the atom starting in its excited state, the exact solution for the mean atomic inversion is given by [9]

$$\langle S_z(t) \rangle_n = \tfrac{1}{2} \cos(2gt\sqrt{n+1}) . \quad (3.6)$$

Then from (3.2) the mean $\langle S_z \rangle_{Y,M}$ in the generalized geometric state is given by

$$\langle S_z(t) \rangle_{Y,M} = \tfrac{1}{2} \sum_{n=0}^{M} P_n(|Y|) \cos(2gt\sqrt{n+1}) , \quad (3.7)$$

where

$$P_n(|Y|) = |Y|^n \left[\frac{1-|Y|}{1-|Y|^{M+1}} \right] . \quad (3.8)$$

The expression (3.7) does not depend on the phase ψ of the parameter Y.

Note that (3.8) is actually valid for an atom initially in its ground or excited state, $\langle S_z(0) \rangle = \pm \frac{1}{2}$. For other initial conditions the solution (3.8) would have an additional term dependent on $\langle S_z(0) \rangle$ which is not zero for such a case, so terms for $(n' \neq n)$ in (3.2') will then contribute.

The numerical results for $\langle S_z(t) \rangle_{Y,M}$ against the normalized time $\tau = 2gt$ are presented in Figs. (4–6). For $|Y| < 1$, namely, $|Y| = 0.5$, $\langle S_z(t) \rangle_{Y,M}$ exhibits more irregular behavior as M increases. The results for $|Y| = 0.95$ are shown in Figs. 5(a) and 5(b). Note that the case for the chaotic-state field is actually realized for values of $M \geq 10$; so for $|Y| \equiv \bar{n}/(1+\bar{n}) = 0.5$, $\bar{n} = 1$, and for $|Y| = 0.95$, $\bar{n} = 19$. Figures 4(b) and 5(b) represent the

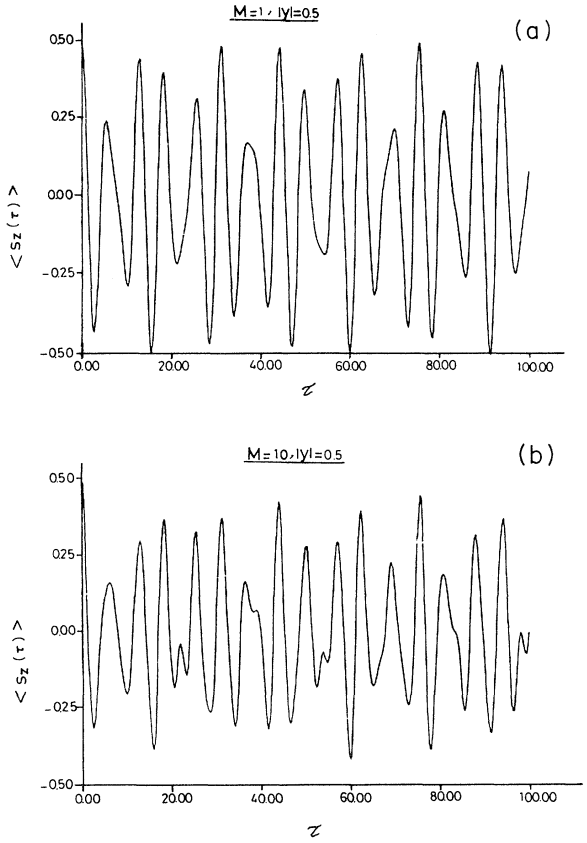

FIG. 4. The atomic inversion $\langle S_z(t) \rangle_{Y,M}$ (in the JC model) against normalized time $\tau = 2gt$ for fixed $|Y| = 0.5$ and (a) for $M = 1$ and (b) $M = 10$.

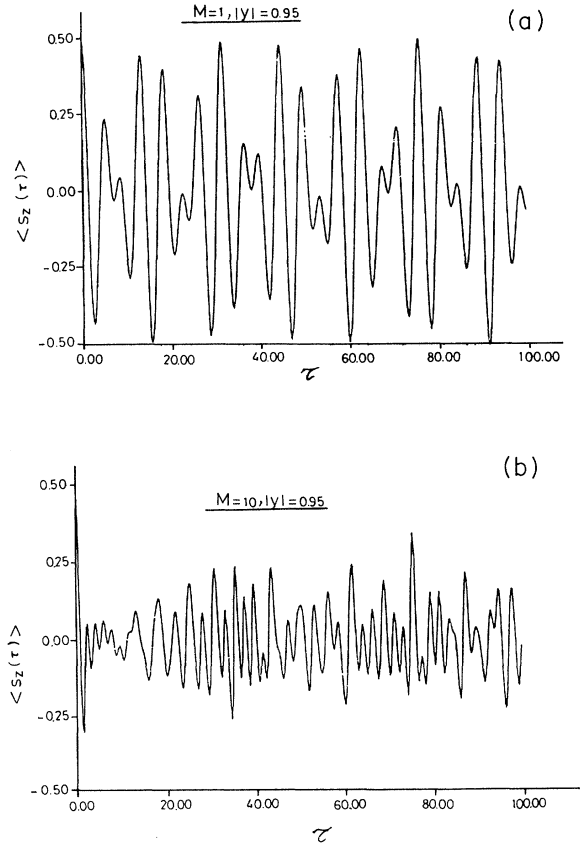

FIG. 5. Same as Fig. 4 but with $|Y| = 0.95$.

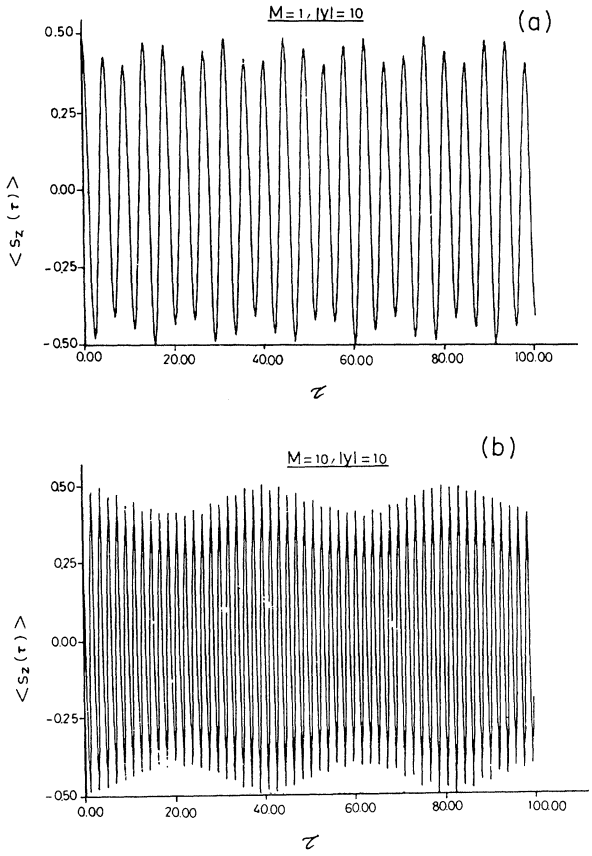

FIG. 6. Same as Fig. 4 but with $|Y|=10$.

cases of relatively weak and strong chaotic fields, respectively, which is in good agreement with the results of Ref. [10].

For higher $|Y|>1$, $\langle S_z\rangle_{Y,M}$ tends to show simple (or regular) oscillations [Figs. 6(a) and 6(b)], as one would expect analytically [Eqs. (3.6), (3.7)] since in this case $|Y,M\rangle \rightarrow$ number state $|M\rangle$ as $|Y|\rightarrow\infty$.

Example 2. Resonance Fluorescence. The phenomenon of resonance fluorescence essentially concerns a two-level atomic system radiatively decaying and coupled to an external radiation field in free space (for example, the atoms can be prepared as an atomic beam). Although exact time-dependent results are available for the single-atom model and both in the case of a single-mode coherent state field [11,12] and in the case of a single-mode number- (Fock) state field [8], we shall be concerned here with the steady-state regime ($t\rightarrow\infty$). In particular, we examine the two cases of the $N=1$ atom and the thermodynamic limit in the cooperative many-atom system in which $N\rightarrow\infty$.

A. Single atom

The mean atomic inversion for a single two-level atom system in the case of the external field is described as a single-mode number state is given in the steady state by [8,13]

$$\langle S_z(\infty)\rangle_n=-\tfrac{1}{2}\sum_{m=0}^{n}\frac{(-)^m n!}{(n-m)!}(b^2)^m \tag{3.9}$$

$$=-(b^2)^n L_n^{(-n-1)}(-b^{-2})\ , \tag{3.9'}$$

where $b^2=2\hbar^{-2}g^2/(\delta^2+\frac{1}{4}\gamma^2)$; g is the coupling constant, γ is the A coefficient, δ is the frequency detuning between that of the external field and of the atom, and $L_n^{(a)}(x)$ is the generalized Laguerre polynomial (see, e.g., [14]). In the generalized geometric state, we then have

$$\langle S_z(\infty)\rangle_{Y,M}=\sum_{n=0}^{M}P_n(|Y|)\langle S_z(\infty)\rangle_n \tag{3.10}$$

and $P_n(|Y|)$ is given by (3.8).

The formula (3.10) for a single atom is plotted in Fig. 7 where for increasing $M=2$ to 20, $\langle S_z(\infty)\rangle$ reaches its steady value at slower rate as $|Y|$ increases in the interval $0\le|Y|<1$.

In the limit $M\rightarrow\infty$ and for $|Y|=\bar{n}/(1+\bar{n})<1$ the formula (3.10) gives

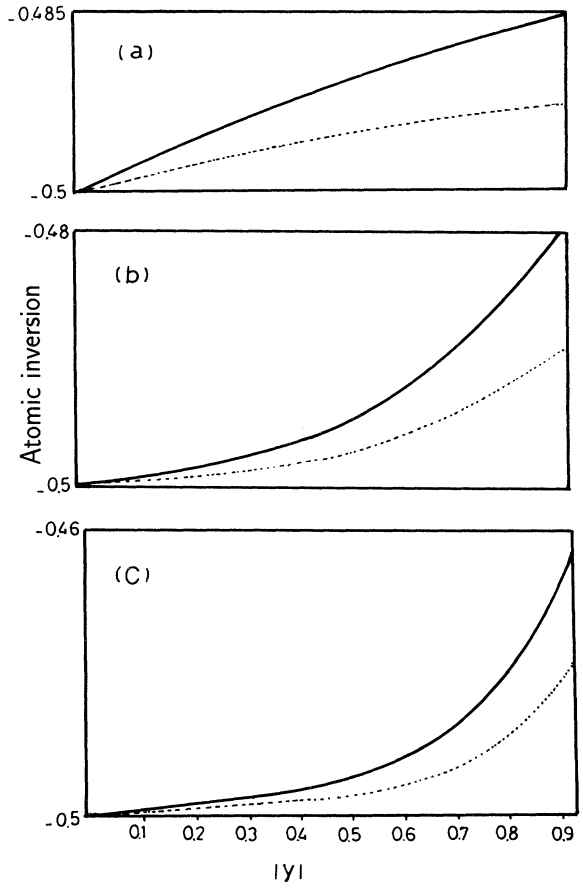

FIG. 7. Atomic inversion $\langle S_z(\infty)\rangle_{Y,M}$ (full line) for $N=1$ atom (with $b^2=10^{-2}$, Eq. (3.10), against $|Y|$ $(0\le|Y|<1)$ (a) for $M=2$, (b) $M=10$, and (c) $M=20$. The dashed line represents the scaled atomic inversion with $X^2=10^{-2}$, Eq. (3.15), in the limit $N\rightarrow\infty$.

$$\lim_{M\to\infty}\langle S_z(\infty)\rangle_{Y,M}=-\tfrac{1}{2}\sum_{n=0}^{\infty}\frac{(\bar{n})^n n!}{(1+\bar{n})^{1+n}}\sum_{m=0}^{n}\frac{(-b^2)^m}{(n-m)!} \tag{3.11}$$

$$=-\left[\frac{1}{1+\bar{n}}\right]\sum_{n=0}^{\infty}\left[\frac{b^2\bar{n}}{1+\bar{n}}\right]^n \times L_n^{(-n-1)}(-b^{-2}) \tag{3.11'}$$

$$\simeq-\frac{1}{(1+\bar{n})}\frac{\exp\{b^2[\bar{n}/(1+\bar{n})]\}}{1+b^2\bar{n}/(1+\bar{n})}\ , \tag{3.12}$$

where the formula (3.12) is valid for $b^2\bar{n}/(1+\bar{n})<1$ (see Ref. [14]).

The formula (3.11) is an alternative form of the derived result [using the p representation form, Eq. (1.1)] for the single-mode chaotic-state field [13,15,16]

$$\langle S_z(\infty)\rangle_{\rm ch}=-\tfrac{1}{2}(b^2\bar{n})^{-1}[\exp(b^2\bar{n})^{-1}]E_1((b^2\bar{n})^{-1})\ , \tag{3.13}$$

where $E_1(x)=\int_x^{\infty}e^{-v}dv/v$ is the exponential integral.

B. The thermodynamic limit ($N\to\infty$)

In the case of N cooperative atomic resonance fluorescence and in the limit $N\to\infty$ [with (γN) kept fixed, so $\gamma\to 0$], the scaled atomic inversion at exact resonance in the number-state field is proved to be [8]

$$\lim_{N\to\infty}\left[\frac{\langle S_z(\infty)\rangle_n}{N}\right]=-\tfrac{1}{2}C_n(\tfrac{1}{2};X^2)$$

$$=-\tfrac{1}{2}\sum_{m=0}^{n}\begin{bmatrix}\frac{1}{2}\\ m\end{bmatrix}\begin{bmatrix}n\\ m\end{bmatrix}m!(-X^{-2})^m\ , \tag{3.14}$$

where $X^2=\gamma N/(2\hbar^{-2}g^2)$ and C_n are the Poisson-Charlier polynomials. Thus in the generalized geometric state

$$\lim_{N\to\infty}\left[\frac{\langle S_z(\infty)\rangle_{Y,M}}{N}\right]=-\tfrac{1}{2}\sum_{n=0}^{M}P_n(|Y|)C_n(\tfrac{1}{2};X^2)\ . \tag{3.15}$$

The case of the chaotic-state field is then obtained by letting $|Y|=\bar{n}/(1+\bar{n})$, $M\to\infty$:

$$\lim_{N\to\infty}\left[\frac{\langle S_z(\infty)\rangle_{\rm ch}}{N}\right]=-\tfrac{1}{2}\sum_{n=0}^{\infty}\frac{(\bar{n})^n}{(1+\bar{n})^{n+1}}C_n(\tfrac{1}{2};X^2)\ . \tag{3.16}$$

The scaled atomic inversion in the limit $N\to\infty$, Eq. (3.15), is shown also in Fig. 7 where the same conclusion applies as in the single-atom case, but with lesser saturation value.

As $M\to\infty$ [case of chaotic-state field, Eq. (3.16) for

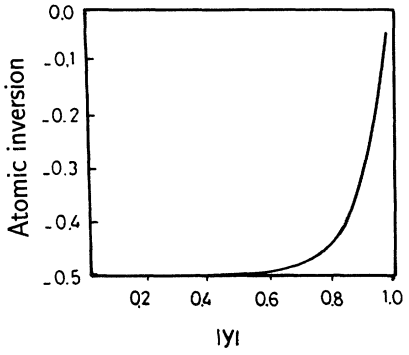

FIG. 8. The scaled atomic inversion in the limit $N\to\infty$ in the chaotic-state field, Eq. (3.16), against $|Y|$ (<1).

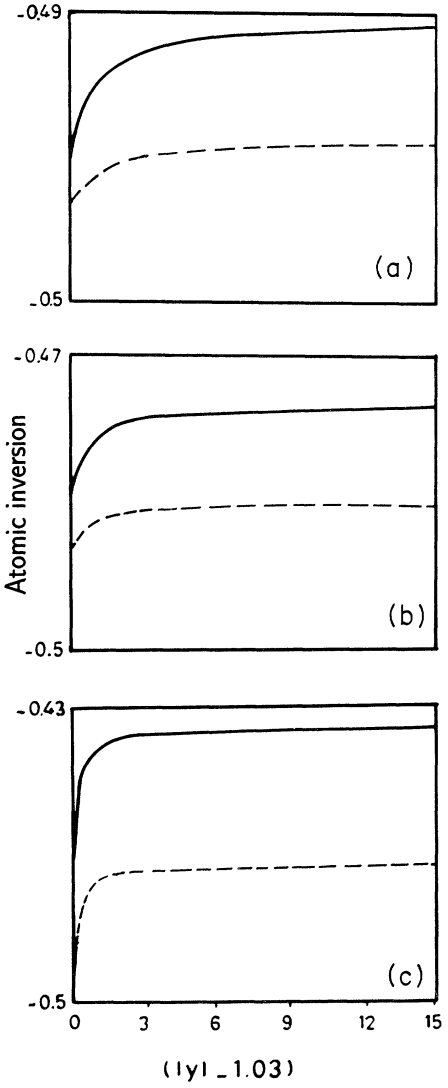

FIG. 9. Same as Fig. (7) but against $|Y|$(>1) (a) for $M=2$, (b) $M=5$, and (c) $M=15$.

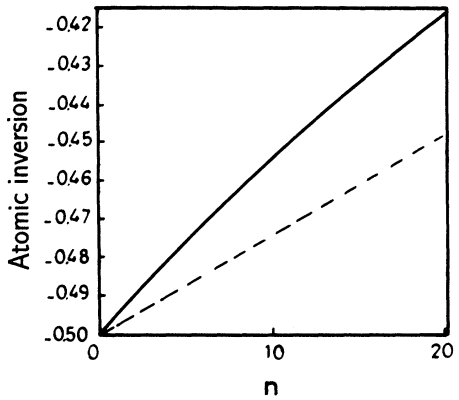

FIG. 10. Atomic inversions Eqs. (3.9), (3.14) for $N=1,\infty$ cases in the number field state $|n\rangle$ against the photon number n. The full line is for $N=1$, the dashed line is for $N=\infty$.

$N\rightarrow\infty$] is shown in Fig. 8 where the behavior is in conformity with the results obtained for finite $N\leq 10$ cooperative atoms [15]: the reach to the value of $\lim_{N\rightarrow\infty}(\langle S_z(\infty)\rangle/N)\simeq 0$ is very slow and requires larger values of $Y=\bar{n}/(\bar{n}+1)$ ($\simeq 0.9$). Now, for comparison with the Fock state field, the behavior of the atomic inversion for the single atom ($N=1$) and in the limit $N\rightarrow\infty$, Eqs. (3.10), (3.15), respectively, are shown in Fig. 9 for $|Y|>1$: As $|Y|\gg 1$ the atomic inversion values for different M are as follows:

M	Eq. (3.10)	Eq. (3.15)
2	−0.491	−0.495
5	−0.476	−0.485
15	−0.436	−0.469

These values are in excellent agreement with the formulas (3.9) and (3.14) for the atomic inversions in the Fock field state representation for $N=1,\infty$ cases, respectively (Fig. 10).

IV. QUASIPROBABILITY DISTRIBUTION FUNCTION

From the earlier work by Wigner [17] and Cahill and Glauber [18] it is well known that the quasiprobability functions are important for the statistical description of a microscopic system and provide insight into the nonclassical features of radiation fields. Therefore we shall turn our attention in this section to the quasiprobability phase space distributions to examine the state given by Eq. (2.1). There are three types of quasiprobability distribution, P representation, W (Wigner), and Q functions. To find these functions we have to calculate the characteristic function $C_p(\zeta)$.

$$C_p(\zeta)=\mathrm{Tr}[\hat{\rho}\exp(\zeta a^{\dagger})\exp(-\zeta^* a)] , \tag{4.1}$$

where $\hat{\rho}$ is the density matrix of the state (2.1),

$$\hat{\rho}=|Y,M\rangle\langle Y,M| . \tag{4.2}$$

From Eq. (2.1), (4.1), and (4.2) after averaging over the phase ψ we have

$$C_p(\zeta)=|\lambda_0|^2\sum_{n=0}^{M}|Y|^n L_n(|\zeta|^2) , \tag{4.3}$$

where $L_n(Z)$ is the Laguerre polynomial defined as

$$L_n(Z)=\sum_{r=0}^{n}\frac{(-)^r Z^r n!}{(r!)^2(n-r)!} . \tag{4.4}$$

Note that, in the limit where $M\rightarrow\infty$, $|Y|<1$ (chaotic state) the characteristic function (4.3) takes the form

$$C_p(\zeta)=\exp\left[-|\zeta|^2\frac{|Y|}{1-|Y|}\right] . \tag{4.5}$$

Having obtained the characteristic function, we are therefore in position to calculate the P representation, W (Wigner), and Q functions.

The P representation affords a convenient way of evaluating the ensemble averages of normally ordered operators and is given by

$$P(\alpha)=\frac{1}{\pi^2}\int_{-\infty}^{\infty}d^2\zeta\exp(\alpha\zeta^*-\alpha^*\zeta)C_p(\zeta) . \tag{4.6}$$

If we insert Eq. (4.3) into Eq. (4.6) we find P is highly singular. This is due to the nonclassical character of the state (2.1). Note that by inserting Eq. (4.5) into Eq. (4.6) one finds the familiar Gaussian form,

$$P(\alpha)=\frac{1}{\pi^2\bar{n}}\exp\left[-\frac{|\alpha|^2}{\bar{n}}\right] , \quad |Y|=\frac{\bar{n}}{1+\bar{n}}<1 . \tag{4.7}$$

Similarly we can calculate the Wigner function W from the equation

$$W(\alpha)=\frac{1}{\pi^2}\int_{-\infty}^{\infty}d^2\zeta\, C_w(\zeta)e^{(\alpha\zeta^*-\zeta\alpha^*)} , \tag{4.8}$$

where $C_w(\zeta)$ is the characteristic function given by

$$C_w(\zeta)=|\lambda_0|^2\sum_{n=0}^{M}|Y|^n L_n(|\zeta|^2)e^{-1/2|\zeta|^2} . \tag{4.9}$$

From Eqs. (4.8) and (4.9) we have

$$W(\alpha)=\frac{2}{\pi}|\lambda_0|^2\sum_{n=0}^{M}(-)^n|Y|^n L_n(4|\alpha|^2)e^{-2|\alpha|^2} . \tag{4.10}$$

In the chaotic state where $M\rightarrow\infty$, $|Y|<1$ we get

$$[W(\alpha)]_{\mathrm{ch}}=\frac{1}{\pi}(\bar{n}+\tfrac{1}{2})^{-1}\exp[-(\bar{n}+\tfrac{1}{2})^{-1}|\alpha|^2] . \tag{4.11}$$

Figures (11–13) show the Wigner function $W(\alpha)$ as a function of $\alpha\equiv\mathrm{Re}(\alpha)+i\,\mathrm{Im}(\alpha)$ for different values of M and $|Y|$. From (4.10) it is clear that $W(\alpha)$ is a symmetric function in both $\mathrm{Re}(\alpha)$ and $\mathrm{Im}(\alpha)$. For $|Y|=0.1$, $W(\alpha)$ is insensitive to M and its Gaussian-like form has its peak at $\mathrm{Re}(\alpha)=\mathrm{Im}(\alpha)=0$ (Fig. 11). As α increases (Figs. 12 and 13) and for $M=1,2$, $W(\alpha)$ exhibits a hole, at the top. As M increases, a peak value of $W(\alpha)$ emerges at its center and eventually $W(\alpha)$ behaves as a Gaussian similar to that of the chaotic state. In all cases $W(\alpha)$ is positive for $|Y|<1$.

As for $|Y|>1$ and for increasing M the presence of the Laguerre polynomial terms in Eq. (4.10) is more effective

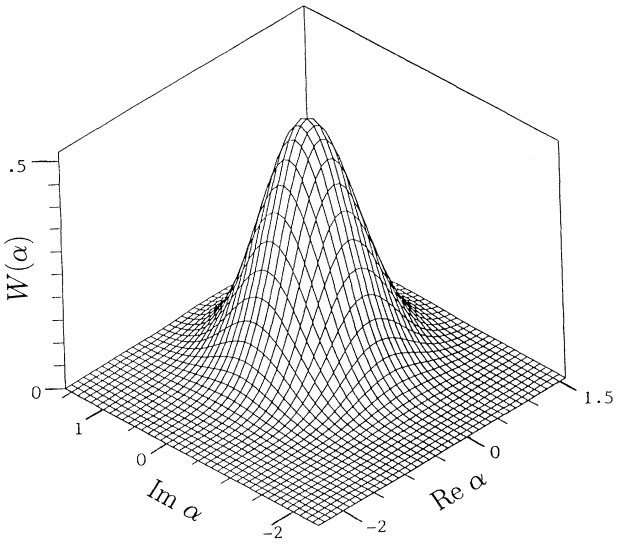

FIG. 11. Wigner function $W(\alpha)$ for $|Y|=0.1$, $M=1$ (same plot is obtained for $M \leq 20$).

and hence $W(\alpha)$ becomes negative around its center (Fig. 14). In fact, Eq. (4.10) reduces to that for a number (Fock) state $|M\rangle$, namely, in the limit $|Y| \gg 1$ and for fixed M,

$$[W(\alpha)]_{\text{Fock}}=\frac{2}{\pi}(-)^M L_M(4|\alpha|^2)e^{-2|\alpha|^2}, \tag{4.12}$$

which tends to zero for $|\alpha| \gg 1$.

Finally we calculate the Q function, which can be used to express the ensemble averages of antinormally ordered operators as a simple integral, that is

$$Q(\alpha)=\frac{|\lambda_0|^2}{\pi^2}\int_{-\infty}^{\infty} d^2\xi \sum_{n=0}^{M} |Y|^n L_n(|\xi|^2)e^{-|\xi|^2+\alpha\xi^*-\xi\alpha^*} . \tag{4.13}$$

Evaluating the integral in Eq. (4.13) yields

$$Q(\alpha)=\frac{|\lambda_0|^2}{\pi}\sum_{n=0}^{M} |Y|^n \frac{|\alpha|^{2n}}{n!}e^{-|\alpha|^2} \tag{4.14}$$

or equivalently,

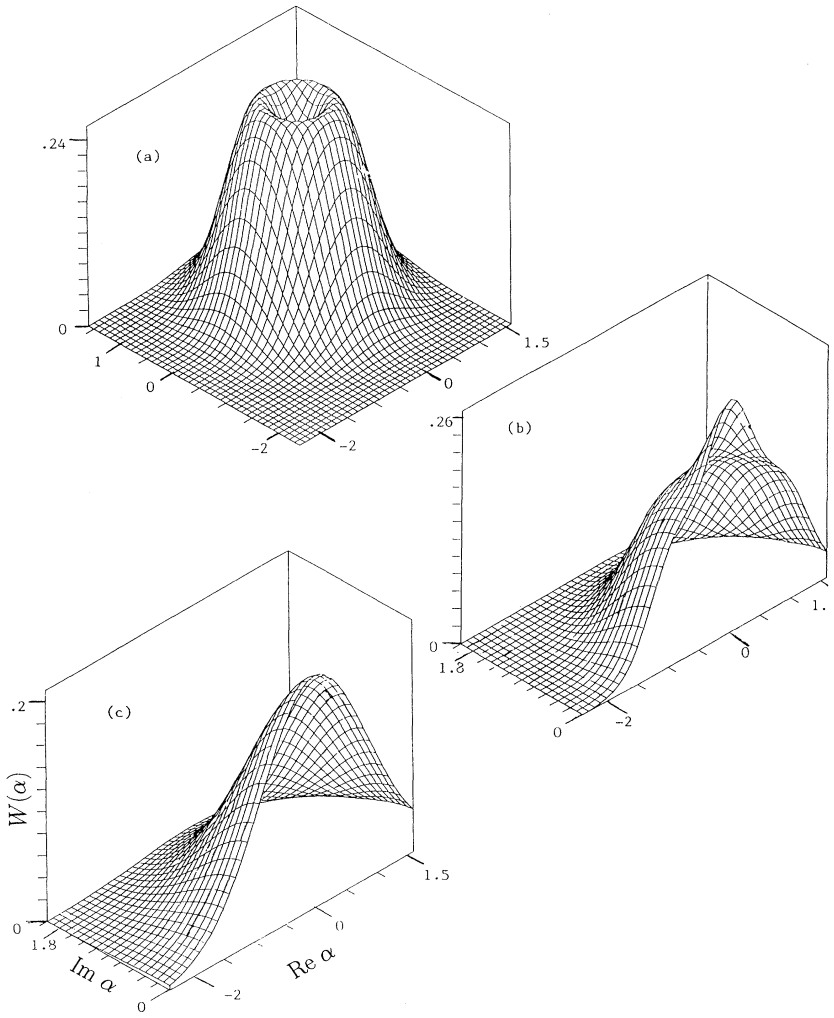

FIG. 12. Same as Fig. 11 but for $|Y|=0.5$ and $M=1,2,20$, (a)–(c), respectively.

$$Q(\alpha)=\frac{|\lambda_0|^2}{\pi}\frac{(-)^M}{M!}L_M^{-M-1}(|\alpha|^2|Y|)\exp(-|\alpha|^2)\ . \tag{4.14'}$$

when M tends to infinity and $|Y|<|$, we have the corresponding formula of the Q function in the chaotic state,

$$[Q(\alpha)]_{\rm ch}=\frac{1}{\pi}(\bar{n}+1)^{-1}\exp[-(\bar{n}+1)^{-1}|\alpha|^2]\ . \tag{4.15}$$

With this we conclude this section and look for a production scheme in the following section.

V. A PRODUCTION SCHEME

Generalizations to the JC model that include nonlinear interactions (in boson and spin variables) have been proposed recently [19]. An interaction Hamiltonian for one of these generalizations that describes multiphoton processes in finite-level atomic systems is of the form

$$H_{\rm int}=\sum_{j=1}^{2r}\frac{g_j}{j!}\{(aS_+)^j+(a^\dagger S_-)^j\}\ , \tag{5.1}$$

where S_3, S_+, and S_- are the inversion, raising, and lowering operators which describe the atomic systems having $(2S+1)$ states. They satisfy the commutation relations $[S_3,S_\pm]=\pm S_\pm$ and S_3 has the eigenvalues m such that $S_3|m\rangle=m|m\rangle$ where $-S\le m\le S$. The field operators a and $a^\dagger$ satisfy the commutation relation $[a,a^\dagger]=1$. The coupling constants g_j couple the atomic system to the field; finally $r\le S$.

This Hamiltonian produces the JC model for $r=\frac{1}{2}$, $S=\frac{1}{2}$. When $r=\frac{1}{2}$ and $S=\frac{3}{2}$ it gives the model discussed by Senitzky [20]. Several values for S were investigated by Buck and Sukumar [21]. The case for general S and $r=\frac{1}{2}$ is the well-known Dicke model and the Tavis-Cummings model [22] of cooperative two-level atoms. Taking $r=1$ and $S=1$, (5.1) describes a three-level atom in interaction with a single mode in which transitions between neighboring levels are effected by single-photon processes while the transition between the upper and lower levels is effected through a two-photon process; which is a special case of a Hamiltonian considered earlier [23] for the three-level atom system.

The interaction model (5.1) then describes a $(2r+1)$-

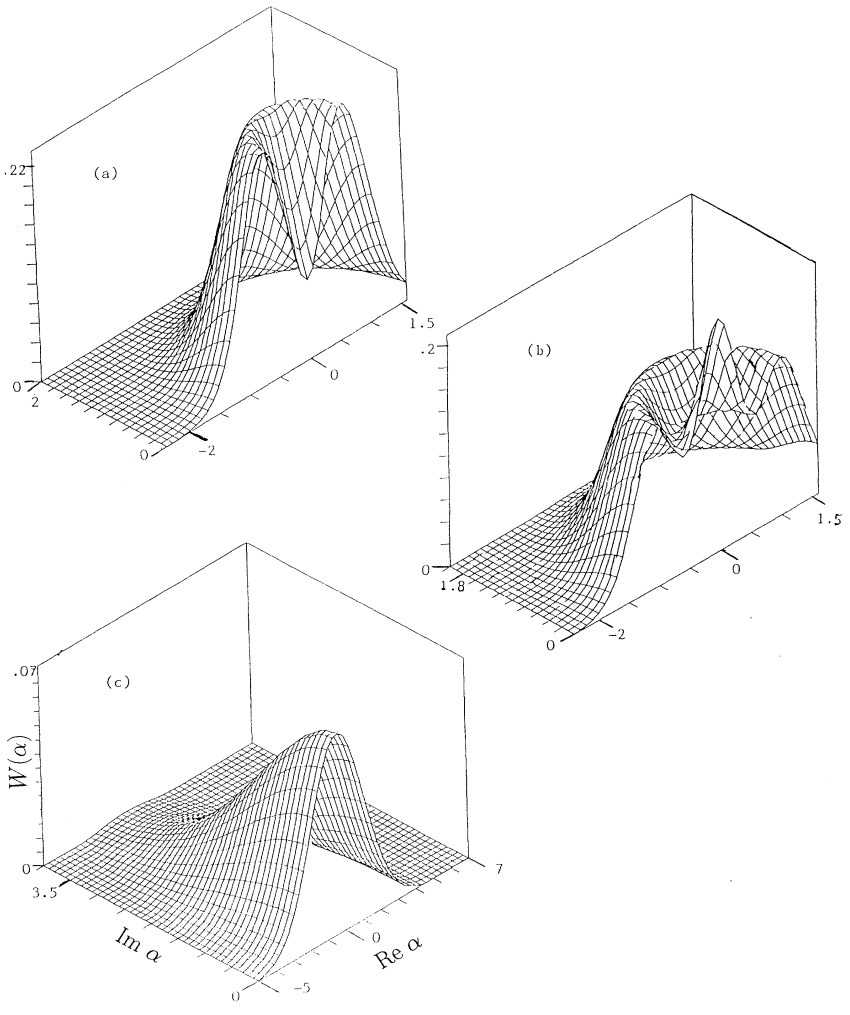

FIG. 13. Same as Fig. 12 but for $|Y|=0.8$.

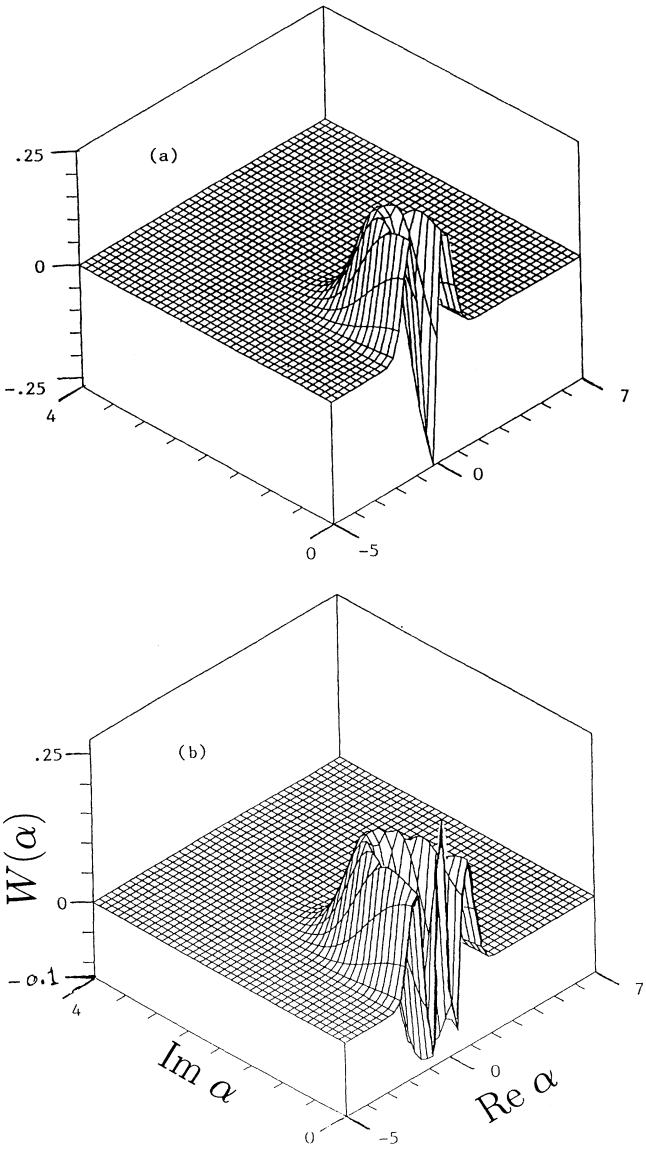

FIG. 14. Same as Fig. 11 for $|Y|=3$, $M=1,2$ [(a),(b), respectively].

level atom interacting with one mode of the radiation field where one-photon transitions occur between neighboring levels, two-photon transitions occur between levels as indicated in Fig. 15 and so on where $2r$-photon transitions occur between the two extreme levels of the atom. The model (5.1) can be used to describe some processes such as multiphonon transitions in a two-level atomic system, multiphonon lasers, and Raman and hyper-

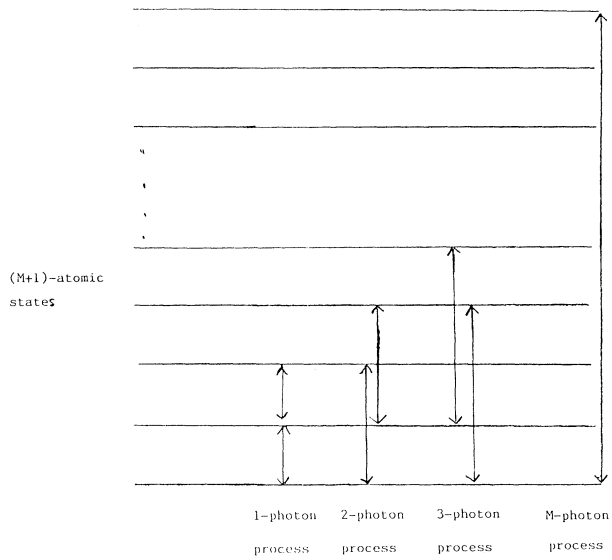

FIG. 15. Diagram symbolizing multiphoton processes in $(M+1)$-atomic level system according to Hamiltonian (5.1).

Raman processes (see references in [19]).

The operators $S_{\pm}^{j}$ when applied to the state vector $|m\rangle$, for which $r=S$, give

$$S_{+}^{j}|m\rangle=\left\{\frac{(S-m)!(S+m+j)!}{(S-m-j)!(S+m)!}\right\}^{1/2}|m+j\rangle\ , \tag{5.2a}$$

$$S_{-}^{j}|m\rangle=\left\{\frac{(S-m+j)!(S+m)!}{(S-m)!(S+m-j)!}\right\}^{1/2}|m-j\rangle\ . \tag{5.2b}$$

We assume that the system is evolving under the Hamiltonian (5.1) from the initial state

$$|\psi(0)\rangle=|0\rangle_{\rm ph}|\vartheta,\Phi\rangle\ , \tag{5.3a}$$

where $|0\rangle_{\rm ph}$ is the vacuum state for the field and

$$|\vartheta,\Phi\rangle=\sum_{m=-S}^{S}\begin{bmatrix}2S\\ m+S\end{bmatrix}^{1/2}\frac{\tau^{m+S}}{(1+|\tau|^2)^S}|m\rangle\ , \tag{5.3b}$$

with $\tau=\tan(\vartheta/2)e^{i\Phi}$, as the atomic coherent state. For a short time t (i.e., $g_j t\ll 1$), the wave function of the system becomes

$$|\psi(t)\rangle=|\psi(0)\rangle-it\sum_{j=1}^{2r}\frac{g_j}{j!}\{(a^{\dagger}S_{-})^j+(aS_{+})^j\}|\psi(0)\rangle\ . \tag{5.4}$$

Using the form (5.3) for $|\psi(0)\rangle$ and the relations (5.2) we get

$$|\psi(t)\rangle=|\psi(0)\rangle-it\sum_{j=1}^{2r}\frac{g_j}{\sqrt{j!}}|j\rangle_{\rm ph}\sum_{m=-S}^{S}\begin{bmatrix}2S\\ m+S\end{bmatrix}\frac{\tau^{m+S}}{(1+|\tau|^2)^S}j!\left\{\begin{bmatrix}S+m\\ j\end{bmatrix}\begin{bmatrix}S-m-j\\ j\end{bmatrix}\right\}^{1/2}|m-j\rangle\ . \tag{5.5a}$$

Suppose at time t the atom is measured to be in its ground state $|-S\rangle$, then the state of the field is given by

$$|\psi_F\rangle \cong \lambda_0|0\rangle - it\sum_{j=1}^{2r}\sqrt{j!}g_j\frac{\tau^j}{(1+|\tau|^2)^S}\begin{bmatrix}2S\\ j\end{bmatrix}|j\rangle\ , \qquad (5.5b)$$

where $\lambda_0=(\cos\vartheta/2)^{2S}$. By taking the coupling constants $g_j\alpha(2S-j)!\sqrt{j!}Y^{j/2}$ and $2r=M$ [i.e., $(M+1)$-level atom] the field state is then the $|Y,M\rangle$ of Eq. (2.1).

VI. SUMMARY

Experiments to prepare pure number states of the field have been recently discussed [24]. Interpolation between the pure number state and the coherent state is done through the binomial state [4]. The generalized geometric state presented in this article bridges between the pure number state and the chaotic state. A single-mode chaotic distribution [Eq. (2.4)] is obtained through averaging over a random phase. There is no need to invent additional dynamical systems or expanding Hilbert spaces as in the case of the thermofield formalism [25].

Properties of the generalized geometric state $|Y,M\rangle$ have been discussed. For $M=2$, the state shows sub-Poissonian statistics for a part of the range, $0.37<|Y|<0.9$. Chaotic behavior starts to appear as we increase M and persists for almost the whole range of $|Y|<1$ and $M=100$. Squeezing effects are shown for some value of M and for $|Y|<1$. It is found that as M increases the maximum amount of squeezing increases. Also the dependence on the phase angle ϕ is shown explicitly. However, for $|Y|\gg 1$ squeezing is lost in conformity with the fact that as $|Y|\to\infty$ the Fock state results.

Two quantum systems have been considered for the interaction with a field in the state $|Y,M\rangle$. The atomic inversion in the JC model shows irregular oscillations. The results for $M=10$ and $|Y|<1$ are in good agreement with earlier results for chaotic fields [10]. Almost simple Rabi oscillations are shown for $|Y|\gg 1$ in accordance with number-state behavior. On the other hand, a single-atom resonance fluorescence shows slow approach to the steady-state value as $|Y|$ increases in the range $|Y|<1$ and M increases from 2 to 20. Also the thermodynamic limit has been discussed and similar conclusions have been drawn, but with lesser values of saturation.

Also, we have shown that the quasiprobability function, the P function of fields in such a state, is singular. The Wigner and the Q functions were also examined.

A production scheme for the generalized geometric state is presented. It depends on nonlinear interactions with an extended JC model [19]. The atomic state is prepared initially in an atomic coherent state, while the field is in the vacuum state. After a short time with the nonlinear interaction the atom is detected in its ground state. The resulting state of the field with suitable choice of the coupling constants is the generalized geometric state. For example, the state $|Y,M=2\rangle$ can be produced using three-level atomic systems in which both one- and two-photon transition processes occur.

*Present address: Dept. of Mathematics, Faculty of Science, Kuwait University, P.O. Box 5969, S'afat 13060, Kuwait.

[1] P. A. M. Dirac, *Principles of Quantum Mechanics*, 4th ed. (Oxford University Press, Oxford, 1958).
[2] R. Glauber, Phys. Rev. **130**, 2529 (1963).
[3] J. Perina, *Coherence of Light* (Reidel, Dordrecht, 1985).
[4] D. Stoler, B. E. Saleh, and M. C. Teich, Opt. Acta **32**, 345 (1985).
[5] G. Dattoli, J. Gallardo, and A. Torre, J. Opt. Soc. Am. B **4**, 185 (1987).
[6] A. Joshi and S. V. Lawande, Opt. Commun. **70**, 21 (1989); J. Mod. Opt. **38**, 2009 (1991); G. S. Agarwal, Phys. Rev. A **45**, 1787 (1992).
[7] C. L. Mehta, Phys. Rev. Lett. **18**, 752 (1967).
[8] S. S. Hassan, R. K. Bullough, and R. R. Puri, Physica A **163**, 625 (1990).
[9] E. T. Jaynes and F. W. Cummings, Proc. IEEE **51**, 89 (1963).
[10] P. L. Knight and P. M. Radmore, Phys. Lett. **90A**, 342 (1982).
[11] B. R. Mollow, Phys. Rev. **188**, 1969 (1969).
[12] S. S. Hassan and R. K. Bullough, J. Phys. B **8**, L147 (1975).
[13] S. S. Hassan, Ph.D. thesis, University of Manchester, 1976 (unpublished).
[14] E. R. Hansen, *A Table of Series and Products* (Prentice-Hall, Englewood Cliffs, NJ, 1975), pp. 89, 318.
[15] S. S. Hassan, G. P. Hildred, R. R. Puri, and R. K. Bullough, J. Phys. B **15**, 2635 (1982).
[16] S. S. Hassan and R. K. Bullough, Physica A **151**, 397 (1988).
[17] E. Wigner, Phys. Rev. **40**, 749 (1932); Z. Phys. Chem. B **19**, 203 (1932).
[18] K. E. Cahill and R. J. Glauber, Phys. Rev. **177**, 1857 (1969); **177**, 1882 (1969).
[19] E. A. Kochetov, J. Phys. A **20**, 2433 (1987).
[20] I. R. Senitzky, Phys. Rev. A **3**, 421 (1971).
[21] B. Buck and C.V. Sukumar, J. Phys. A **17**, 877 (1984); **17**, 885 (1984).
[22] R. H. Dicke, Phys. Rev. **93**, 99 (1954); M. Tavis and F. W. Cummings, *ibid.* **170**, 379 (1968); **188**, 692 (1969).
[23] A. -S. F. Obada and A. M. Abdel-Hafez, J. Mod. Opt. **34**, 665 (1987).
[24] J. Krause, M. O. Scully, T. Walther, and H. Walther; Phys. Rev. A **39**, 1915 (1989); J. Krause, M. O. Scully, and H. Walther; *ibid.* **36**, 4547 (1987).
[25] Y. Takahashi and H. Umezawa; Collect. Phenom. **2**, 55 (1975); S. M. Barnett and P. L. Knight, J. Opt. Soc. Am. B **2**, 467 (1985).